Title

MODULATED STRUCTURES IN (Cu-Mn)3Al ALLOYS II. FORMATION OF AN Llo PHASE WITHIN THE Cu3Al-SIDE PHASE

Authors

Bouchard, M.
Thomas, G.

Publication Date

1973-11-01

LBL-2295
Preprint c.2

MODULATED STRUCTURES IN $(Cu\text{-}Mn)_3Al$ ALLOYS II. FORMATION OF AN $L1_0$ PHASE WITHIN THE Cu_3Al-SIDE PHASE

M. Bouchard and G. Thomas

November 1973

Prepared for the U. S. Atomic Energy Commission
under Contract W-7405-ENG-48

DISCLAIMER

LBL-2295

MODULATED STRUCTURES IN $(Cu\text{-}Mn)_3Al$ ALLOYS

II. FORMATION OF AN $L1_o$ PHASE WITHIN THE Cu_3Al-SIDE PHASE

M. Bouchard* and G. Thomas

Department of Materials Science and Engineering,
College of Engineering and Inorganic Materials Research Division,
Lawrence Berkeley Laboratory, University of California,
Berkeley, California 94720

ABSTRACT

Alloys along the composition tie-line Cu_3Al-Cu_2MnAl decompose inside a miscibility gap by forming composition modulations rich in the Cu_3Al and Cu_2MnAl. At temperatures near the misicibility gap, the Cu_3Al-side modulations possess the DO_3 structure whereas at temperatures well inside the miscibility gap, the structure becomes that of L_o. The results are interpreted in terms of an L_o phase field within the binary-rich end of the miscibility gap. The proposed L_o phase results from the ordering of one set of {220} planes of the ordered matrix. There are twelve possible L_o variants that can be classified into three sets of twin related variants coherent with their anitphase related counterparts. The two twin related variants concurrently grow in platelets parallel to the {100} plane of the matrix that contains the two C axes. The antiphase related variants are believed to form a long period superlattice. In alloys aged near the top of the miscibility gap, the Cu_3Al-rich phase possesses a tweed-like texture which suggests the presence of a device array of small L_o particles coherent with the DO_3 matrix.

*Present address: Communication Research Center, P. O. Box 490, Station A
Ottawa, Canada

1. INTRODUCTION

The alloys along the composition-line Cu_3Al-Cu_2MnAl isothermally decompose inside a miscibility gap into a Cu_3Al-rich phase and a Cu_2MnAl-rich phase. The metallographic characteristics of the alloys decomposed at tempertures close to the miscibility gap are described in paper I. At temperatures well inside the miscibility gap, electron diffraction and microscopy reveal the presence of a new phase having a structure which appears to be that of LI_o (Cu-Au I type).

The present paper discusses the formation of the LI_o phase during isothermal aging inside the miscibility gap.

2. EXPERIMENTAL

The experimental procedure has been described in paper I and the compositions of the alloys studied have been given in Table I of the former paper.

3. RESULTS

3.1. The Ll_o Phase

The diffraction patterns of alloys aged well inside the miscibility gap show extra reflections, whose diffuseness increases with increasing aging temperature (240°C to 300°C). Typical examples of discrete and diffuse extra reflections in alloy 0.8 are shown in Figs. 1 and 2 respectively. A comparison of Figs. 2a and b reveals that the intensity of the extra reflections in the (001) diffraction pattern increases when the foil is slightly tilted from the exact (001) orientation, and such tilting experiments are necessary to determin the distribution of the extra reflections in the reciprocal space. It was found that the structure of the new phase was best fitted to that of the Ll_o superstructure (the Cu-Au I structure) and this new phase will be called the Ll_o phase in this paper.

Figure 1a,b shows the (011) and the (110) diffraction patterns from the alloy 0.8 aged at 240°C for 10,000 min. The diffraction patterns contain matrix and precipitate reflections and the latter are indexed in Fig. 1c,d terms of the proposed Ll_o structure. Selected dark field experiments reveal that the Ll_o reflections in the (001) matrix diffraction pattern in Fig. 1a come from two Ll_o variants having mutually orthogonal c axes. The two variants are marked (1) and (2) in Fig. 2. The LI_o reflections in Fig. 1 are elongated in a direction normal to the c axis of the Ll_o phase. It was also found that the Ll_o reflections in the (110) matrix diffraction pattern in Fig. 1 come from only one Ll_o variant.

The $L1_o$-matrix orientation relationship was determined from many diffraction experiments. The results are schematically shown in Fig. 3. The solid lines indicate the unit cell of the ordered DO_3 matrix and the dashed lines indicate the unit cell of the proposed $L1_o$ phase. The labeling of the Cu and Al atoms in Fig. 3 refers only to the DO_3 structure. The important features of the proposed $L1_o$ phase are summarized as follows:

a) The $L1_o$ structure consists of alternate stacking of A and B {100} planes perpendicular to the (tetragonal) c axis.

b) The c axis of the $L1_o$ phase lies nearly parallel to one of the ⟨110⟩ directions of the matrix, thus producing six possible $L1_o$ variants corresponding to the six ⟨110⟩ directions of the matrix. For example, the c axis of variants (1) and (2) shown in Figs. 1&2 lie near the [220] and the [2$\bar{2}$0] matrix directions respectively. Variants (1) and (2) are twin related and the twin plane is the (100) plane of the matrix. Because of the cubic symmetry, two additional sets of twin related variants have their c axes in the (100) and the (010) planes of the matrix. In addition, each of the six variants can be APB related to another variant possessing the same orientation of its c axis. This produces a total of twelve possible $L1_o$ variants.

c) Measurements from diffraction patterns revealed that there is a near correspondence of atomic positions between the $L1_o$ structure and the matrix structure. The dimensions of the $L1_o$ unit cell estimated from the Cu_2MnAl matrix unit cell are:

$$A = 4.24\ \text{Å}$$

$$B = 2.97\ \text{Å}$$

$$C = 4.24\ \text{Å}$$

The C axis is normal to the AB stacking sequence and does not correspond to the shortest dimension of the unit cell.

It was calculated that for the proposed $L1_o$ structure, the following hkℓ reflections are allowed:

h, k and ℓ unmixed	$F_f = 2(f_A + f_B)\cdots$(fundamental)
h and k unmixed and h, k and ℓ mixed	$F_s = 2(f_A = f_B)\cdots$(superlattice)

where F is the structure factor associated with the hkℓ reflection and f_A and f_B are the electron scattering powers of the A and B atoms (Cu and Al) respectively.

The morphology of the $L1_o$ phase was studied by selected dark field microscopy. The bright field micrograph of the alloy 0.8 aged at 240°C for 10,000 minutes shown in Fig. 4a reveals the preferential polishing near the edge of the foil of a component having a plate-like morphology. The image shows grey dotted contrast believed to be caused by contamination of the sample since it was observed only in one sample. This is consistent with the observation that the dotted contrast does not disappear when the foil is tilted. The dark field micrographs in b) and c) [from the same foil as in a)] were obtained using the $(201)_1$ and $(201)_2$ $L1_o$ reflections in Fig. 1a) and show the variants (1) and (2) respectively. The two dark field micrographs of the same area show that each $L1_o$ variant consists of small elongated particles having their long axes parallel to their respective c axis.

The elongated shape of the particles produces some streaking of the $L1_o$ diffracted spots in directions normal to the c axis.[1] (See Fig. 1a).

The dark field micrographs in Fig. 4b and c also show that the particles of each $L1_o$ variant generally form groups and that the groups of the twin related particles (1) and (2) are located within the same area of the foil. This suggests a highly interconnected arrangement of the twin related particles. It was found that within each group of particles, the space unoccupied by variant (1) in Fig. 4b is partially occupied by variant (2) in Fig. 4c.

The relative volume fractions of each variant differ markedly from area to area in the foil. This is shown in the two dark field micrographs of the alloy 0.8 aged at 240°C for 10,000 minutes in Fig. 5a and b obtained from the same area. The morphology of variant (1) in a can be best described as irregularly shaped platelike particles. The surface of the plates is irregular and contains numerous valleys and hills. Clearly, variant (1) has a larger volume fraction than variant (2) in b. The latter is distributed in a dense array of small particles showing white dotted contrast in a dark field. In fact, the small particles of variant (2) in b are aligned in rows parallel to a ⟨110⟩ direction of the matrix. These rows are located in the valleys of variant (1). This is illustrated by the particles of variant (2) indicated by arrows in b and the corresponding valley in the plate-shaped variant (1) in a.

In [110] foils, normal to the direction of c_1, the particles of variant (1) are clearly seen to be distributed in platelets lying in

the (001) plane of the matrix. The dark field micrograph from a (110) foil in Fig. 6 was obtained using the $Ll_o(110)_1$ reflection in Fig. 1b. The micrograph shows that the platelets parallel to the (001) plane of the matrix are 100-200Å thick and 400-500Å apart. The particles of variant (2) are believed to be located between those of variant (1) and within the same platelet. The areas near the edge of (001) foils may contain only one platelet of the twin related variant (1) and (2). In thicker areas of the foils, overlapping platelets may be observed. The three dimensional distribution of Ll_o particles is best studied by stereo microscopy. The dark field pair of stereo micrographs in Fig. 7 reveal that the particles of one variant are distributed in platelets located at various depths in the sample.

From the above dark field analysis, it is believed that the Ll_o phase form three sets of platelets parallel to the cube planes of the matrix. Each {001} platelet contains the two twin related Ll_o variants with their c axes parallel to the two ⟨110⟩ directions of the matrix that are parallel to the platelets. This three dimensional distribution of the three sets of twin related variants is schematically illustrated in Fig. 8.

There are twelve possible transformation variants generated from the matrix. The twelve variants can be divided into three pairs of twin related variants coherent with their antiphase (AP) related counterparts. The AP related variants share the same direction of their C axes, but their interface is characterized by the wrong stacking sequence of AB planes ABABBABA forming APBS. This situation is similar to that found in Cu-Au and may result in a long period

superlattice LPS.[2] The interface between two APB related variants is a 1/2a (101) or 1/2a (011) APB of the $L1_o$ structure. In dark field micrographs obtained using a superlattice $L1_o$ reflection [e.g. (201)], the APB is expected to show dark contrast since α, the phase angle across the APB = $2\pi g \cdot R = \pi(201)\cdot(101) = \pi$.[3] We believe that the closely spaced dark fringes in the dark field photograph in Fig. 9a is evidence of the LPS in the $L1_o$ phase. The contrast at APB's is very sensitive to the diffraction conditions and the nature of the contrast may change from dark to white by small deviation from the exact Bragg condition,[3] and the contrast of the closely spaced dark fringes vanishes when the foil is tilted. This observation further supports that the fringes are caused by APB contrast inside the $L1_o$ particles. As shown earlier, the wider dark bands are valleys in variant (1) that are at least partially occupied by the twin related variant (2), and consequently this contrast does not vanish when the foil is tilted slightly. It was found that the period of the LPS is constant within each platelet of the $L1_o$ phase, but varies between 60Å to 110Å from platelet to platelet.

In order to determine the component responsible for the appearance of the $L1_o$ phase (Cu_3Al-rich or Cu_2MnAl-rich), the symmetrical alloy 0.5 was first aged at 300°C for 18,000 minutes and further aged at 240°C for 1300 minutes. The first aging produces the double cubic structure whereas at lower temperatures, one of the two components transforms. Two characteristic features of the low temperature transformation were observed. Firstly, the microstructure is characterized

by the presence of a high density of martensite plates shown in Fig. 10a in the phase labelled B. It is believed that these martensite plates are formed in the Cu_3Al-rich phase as this is consistent with previous observations in Cu-Al alloys. The second characteristic feature is observed in small areas of the foil not transformed to martensite (e.g. Fig. 10b). Instead, the component labelled B now shows a modulated structure in bright field similar to that caused by the $L1_o$ structure in asymmetrical alloys. Selected dark field microscopy using the closely spaced spots has shown that the transformed component possess the smaller lattice parameter associated with the Cu_3Al-rich phase. One such experiment is shown in Fig. 11 where the phases labelled A and B are imaged in the dark field micrographs in d and c respectively obtained from the corresponding closely spaced d and c spots in the diffraction pattern in b. This result suggests that at temperatures well inside the miscibility gap, the decomposition proceeds by the formation of compositional modulations of cubic Cu_2MnAl-rich regions coherent with Cu_3Al-rich regions which have the $L1_o$ structure.

3.2. Structure of the Cu_3Al Phase

During aging of the symmetrical alloy 0.5, diffuse streaking and extra diffuse reflections were observed. The image contrast showed "tweed-like" texture. These features are similar to those observed in the as-quenched alloys described in paper I. Typical examples of the (001) diffraction pattern and microstructure of the alloy 0.5 aged at 300°C for 10,000 min are shown in Figs. 2 and 12, (see also Fig. 12 of paper I).

There are two sources of diffuse intensity in diffraction patterns during the early stages of aging. In (001) diffraction patterns, the intersection of some ⟨110⟩ diffuse streaks with the reflecting sphere produces diffuse intensity near the fundamental reflections very similar to the cross patee, see paper I. However, the diffuse cross patee appears around all reflections and its shape is independent of the g vector whereas the diffuse crosses caused by the intersection of the ⟨110⟩ diffuse streaks with the reflecting sphere near the fundamental reflections are more intense than those near the superlattice reflections. Moreover, the size of the latter diffuse crosses increases with increasing order of reflection. This different behavior of the two types of diffuse scattering may be utilized to determine the origin of the diffuse intensity.

Diffuse maxima are resolved along the length of the diffuse streaks. These maxima are centered around the position of the $L1_o$ reflections in reciprocal space. A dark field micrograph obtained using the $(201)_{L1_o}$ reflection in Fig. 2b is shown in Fig. 12b) and compared to the corresponding bright field image in Fig. 12a). The figure reveals that the phase showing the "tweed-like" texture contains a high density of fine coherent particles as evidenced by the white dotted contrast in dark field. Selected dark field microscopy of two closely spaced spots in diffraction patterns of the fully decomposed alloy 0.5 revealed that the component showing the "tweek-like" texture possess the smaller lattice parameter associated with the Cu_3Al-rich phase. This observation and the results given in the previous section suggest that the

"tweed-like" texture and the diffuse streaks and reflections represent a mixture, within the Cu_3Al-rich phase, of small coherent $L1_o$ particles embedded in a cubic DO_3 superstructure. Similar structures have been observed in a number of ordered alloys.[4,5,6]

4. DISCUSSION

The "Tweed-like" Texture and the $L1_o$ Phase

Our results show the existence of a new phase having a structure similar to that of the $L1_o$ structure during the decomposition of the $(Cu\text{-}Mn)_3Al$ alloys at temperatures well inside the miscibility gap. The $L1_o$ structure consists of the alternate stacking of planes of A and B atoms normal to the C axis. The C axis of the $L1_o$ phase lies parallel to one of the ⟨110⟩ directions of the DO_3 transforming crystal. Since we observe little deviation from the exact correspondence of lattice sites between the matrix and the $L1_o$ structure, we have proposed an $L1_o$ structure having its C axis normal to the smallest dimension of the unit cell.

The DO_3-$L1_o$ transformation is one involving transformation of a bcc structure to a fcc structure. We believe that the transforming crystal has a composition and a structure approaching, but different from, that of the Cu_3Al-DO_3 structure, (this is suggested by the rotation of the decomposition tie-line discussed in paper III), and that Mn atoms play an important role in the formation of the $L1_o$ structure. If decomposition inside the miscibility gap is spinodal in nature, it is possible that the composition of the Cu_3Al-rich phase gradually shifts towards the

ternary composition having the $L1_o$ structure. At temperatures below 275°C, the $L1_o$ phase is stable, whereas at 300°C, it is metastable and produces diffuse $L1_o$ reflections and a "tweed-like" or two-phase texture. The "tweed-like" texture of the Cu_3Al-rich component could also be produced during the quench subsequent to the isothermal aging. These observations suggest the presence of a $L1_o$ phase field at the binary-rich end of the miscibility gap.

The proposed structure of the $L1_o$ phase may be generated from the DO_3 structure simply by the partial disordering of the DO_3 lattice to the B2 lattice followed by the ordering of only one set of the {110} planes of the B2 structure. One possible mechanism performing the above transformation is illustrated in Fig. 13. The mechanism involves the generation of non-conservative 1/4 a⟨111⟩ APB's of the DO_3 structure parallel to every (220) planes of the DO_3 structure.[5,7] The condition for non-conservative (UVW) [hkℓ] APB's is

$$[uvw]\cdot[hk\ell] \neq 0$$

where [uvw] is the normal to the palne of the APB and [hkℓ] is the direction of the APB vector. There are four possible 1/4a⟨111⟩ vectors in the DO_3 structure generating four macroscopically equivalent APB's. Since non-conservative APB's are associated with compositional changes at the APB's, closely spaced non-conservative APB's can therefore produce local compositional changes approaching the composition of a new phase. This structural interpretation of phase relations was recently illustrated by Okamoto and Thomas[5] in Ni-Mo alloys. In the DO_3 structure, the two APB's (220) 1/4a [111] and (220)1/4a[11$\bar{1}$] are

SUMMARY

1. At temperatures near the top of the miscibility gap the Cu_3Al-rich and Cu_2MnAl-rich modulations possess the DO_3 and $L2_1$ structures respectively. At lower temperatures, the Cu_3Al-rich modulation also exhibits a tetragonal structure believed to be similar to the $L1_o$ superstructure.

2. At temperatures near the top of the miscibility gap the Cu_3Al-rich modulation shows a "tweed like" texture and correspondingly the diffraction patterns show diffuse streaking and diffuse extra reflections corresponding to those of the $L1_o$ structure. It is suggested that these features arise from a high density of $L1_o$ particles coherent with the DO_3 structure.

3. The formation of the $L1_o$ phase is thought to reflect the presence of a $L1_o$ phase field within the binary-rich end of the miscibility gap.

4. There are twelve possible $L1_o$ variants that can be classified into three sets of twin related variants coherent with their APB related counterparts.

5. The $L1_o$ phase consists of the stacking of A and B planes parallel to a {110} plane of the matrix. The twin related variants concurrently grow in platelets parallel to the {100} planes of the matrix and the twin plane is of the type {100}.

6. The near correspondance of the lattice sites during the DO_3-$L1_o$ transformation produces coherent $L1_o$ particles such that the normals to the {110} AB stacking are perpendicular to the shortest dimension of the unit cell.

7. There are two types of morphologies of the $L1_o$ particles: a) small particles elongated in a direction normal to the AB stocking and b) plate-shape particles parallel to the {100} planes of the matrix.
8. In the plate-shape particles, there are two type of fringes observed. The wider fringes (typically 400-500Å) are valleys in the plates of one variant that are accupied by small elongated particles of the twin related variant. The closer fringes (typically 60-110Å) are believe to reflect the presence of a long period superlattice in the large $L1_o$ particles.
9. The DO_3-$L1_o$ transformation can be accomplished by the ordering of only one set of the {220} type planes in the DO_3 structure. The generation of closely spaced non-conservative 1/4 a ⟨111⟩ APB's is equivalent to the formation of a small $L1_o$ region coherent with the DO_3 structure.

ACKNOWLEDGEMENTS

This work was sponsored by the Atomic Energy Commission through the Lawrence Berkeley Laboratory. M. B. gratefully acknowledges receipt of a fellowship by Hydro-Quebec and SIDBEC-DOSCO, Montreal, Canada. The line diagrams were skillfully drawn by G. Pelatowski.

REFERENCES

1. P. B. Hirsch, A. Howie, R. B. Nicholson, D. W. Poshley and M. J. Whelan, Electron Microscopy of Thin Crystals, (London Butterworths, 1965).

2. H. Sato and R. S. Toth, Alloying Behavior and Effects in Concentrated Solid Solutions, T. B. Massalski ed., Gordon and Breach, Science Publishers Inc., New York (1965).

3. M. J. Marcinkowski, Electron Microscopy and Strength of Crystals, (Interscience N.Y. 1962) G. Thomas and J. Washburn, ed.

4. H. Sato, R. S. Toth and G. Hondo, J. Phys. Chem. Solids, 28, 137 (1967).

5. P. R. Okamoto and G. Thomas, Acta Met., 19, 825 (1971).

6. S. K. Das, P. R. Okamoto, P. M. J. Fisher and G. Thomas, Acta Met. 21, 913 (1973).

7. J. B. Mitchell, Scripta Met. 4, 411 (1970).

FIGURE CAPTIONS

Fig. 1. (001) and (110) matrix diffraction patterns from the alloy $Cu_{2.2}Mn_{0.8}Al$ (x=0.8) aged at 240°C for 10,000 minutes. The extra reflections (in parenthesis) are indexed in terms of the proposed $L1_o$ phase. In a), the two twin related variants (1) and (2) are diffracting whereas in b), only the variant (1) is diffracting. The patterns are induced in c and d.

Fig. 2. (001) diffraction patterns of the alloy $Cu_{2.5}Mn_{0.5}Al$ (x=0.5) aged at 300°C for 10,000 min. and showing diffuse streaking and diffuse $L1_o$ reflections. Note that the diffuse intensity increases when the foil is tilted slightly from the (001) orientation in (b).

Fig. 3. Schematic representation of the coherent lattice relationship between the DO_3 structure and the $L1_o$ structure. The atoms at lattice sites refer only to the DO_3 structure. The c axis of the $L1_o$ phase is normal to its AB stacking sequence and normal to the B axis representing the smallest dimension of the unit cell. It can be seen that the $L1_o$ structure can be generated from the DO_3 structure simply by the ordering of one of the (110) planes of the bcc disordered unit cell.

Fig. 4. Micrographs from the alloy $Cu_{2.2}Mn_{0.8}Al$ aged at 240°C for 10,000 minutes. A typical bright field micrograph is shown in a). The dark field micrographs in b) and c) were obtained using the $(201)_1$ and $(201)_2$ $L1_o$ reflections marked in Fig. 1(a) and show the variants (1) and (2), respectively.

Fig. 5. Same alloy and diffraction contrast as in Fig. 4. The figure reveals that within the same area, the variant (1) in a) has a larger volume fraction than the variant (2) in b). The variant (1) has an irregular plate-like morphology whereas the variant (2) form rows of small particles parallel to the $[1\bar{1}0]$ direction of the matrix. The particles of variant (2) are located within the dark valleys in the platelets of variant (1) (see arrows).

Fig. 6. Dark field micrograph showing the Ll_o variant (1) in a (110) foil of the alloy $Cu_{2.2}Mn_{0.8}Al$ (x=0.8) aged at 240°C for 10,000 minutes. The image was obtained using the (110) Ll_o reflection in Fig. 1(b) and shows that the Ll_o phase grows in platelets parallel to the cubic plane.

Fig. 7. Stereo pair of dark field micrographs obtained using the (201) Ll_o reflection in the alloy $Cu_{2.2}Mn_{0.8}Al$ (x=0.8) aged at 240°C for 10,000 minutes. The three dimensional distribution of particles can be observed using a small portable stereo viewer. The stereo pair reveals that the particles within one group are distributed at various depths in the thin foil.

Fig. 8. Schematic representation showing the three dimensional distribution of the 6 possible twin related Ll_o variants forming platelets parallel to the cube planes in the $Cu_{2.2}Mn_{0.8}Al$ (x=0.8) alloy.

Fig. 9. (201) Ll_o dark field micrographs from the alloy $Cu_{2.2}Mn_{0.8}Al$ (x=0.8) aged at 240°C for 10,000 minutes showing parallel dark fringes (see circles areas) in some areas of the Ll_o plates. A comparison of the circled areas in a) and b) reveals that the fringe contrast vanishes by changing slightly the diffraction conditions. It is believed that the fringes reveal the presence of a long period supperlattice in the Ll_o phase.

Fig. 10. Bright field micrographs of the alloy $Cu_{2.5}Mn_{0.5}Al$ (x=0.5) aged at 300°C for 18,000 minutes and subsequently aged at 240°C for 1300 minutes. The figure shows the transformation of the Cu_3Al-rich component labelled B during the low temperature aging. In the area in a) the Cu_3Al-rich component transforms mostly to martensite whereas in b) it transforms mostly to the Ll_o phase.

Fig. 11. Alloy $Cu_{2.5}Mn_{0.5}Al$ (x=0.5) aged at 300°C for 18,000 minutes and subsequently aged at 240°C for 1300 minutes. The bright field micrograph shows an area of the foil where the component labelled B has transformed to the Ll_o structure. The corresponding dark field micrographs in c) and d) were obtained using the closely spaced c and d reflections respectively marked in b). The figure reveals that the component labelled B possess the smaller lattice parameter associated with the Cu_3Al-rich component.

Fig. 12. (220) bright field micrograph (a) of the alloy $Cu_{2.5}Mn_{0.5}Al$ ($x=0.5$) aged at 300°C for 10,000 min. showing the "tweed-like" texture of the Cu_3Al-rich component labelled B. The corresponding dark field micrograph shwon in (b) was obtained using the diffuse $(201)_{L1_o}$ reflection in Fig. 2(b). Note the presence of the strong white dotted contrast in (b) only in the Cu_3Al-rich component characterized by the "tweed-like" texture.

Fig. 13. Schematic representation of a possible mechanism for the Cu_3Al-$L1_o$ transformation by the generation of parallel non-conservative a/4 ⟨111⟩ APB's at every {220} planes of the DO_3 structure. In (a), the five (001) atomic planes of the DO_3 structure are represented by decreasing the size of atoms lying at various (001) depths. Note that there is no ordering of the {220} planes in the DO_3 structure. The faulted DO_3 structure in (b) is equivalent to the $L1_o$ structure described in the text where the $(2\bar{2}0)$ planes of the DO_3 structure order.

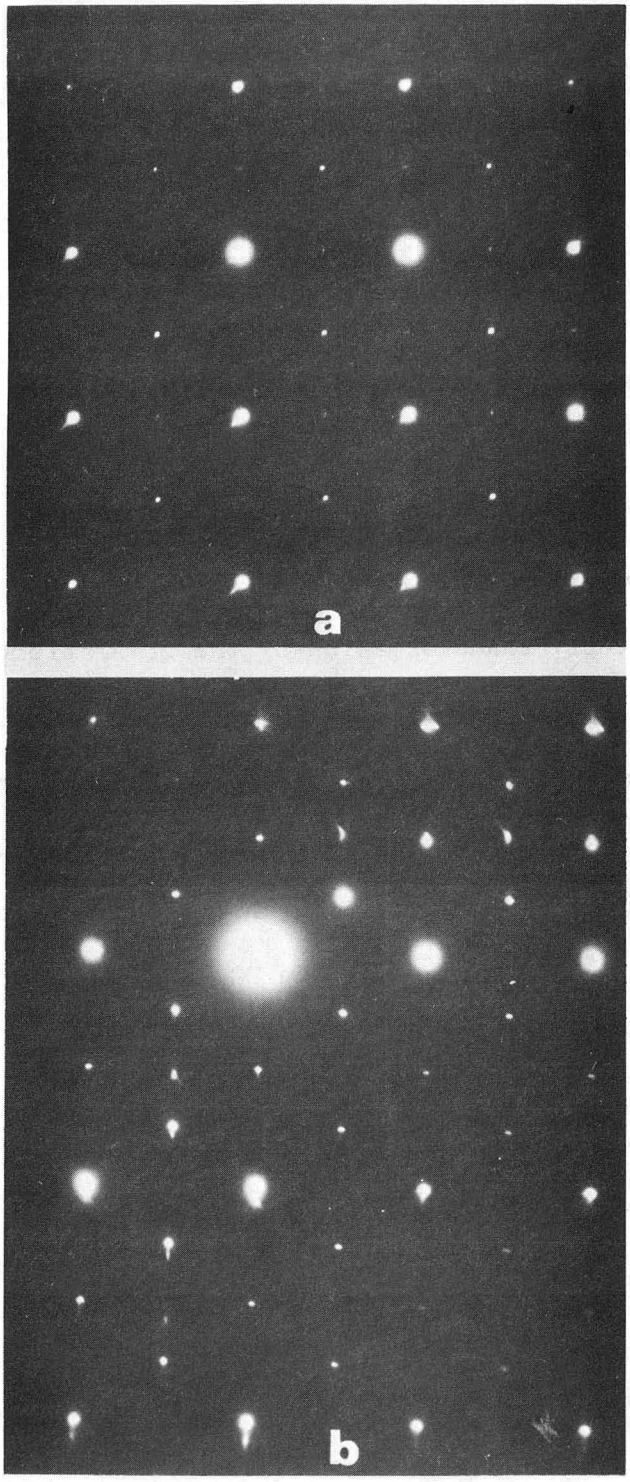

XBB 7211-5721

Fig. 1.

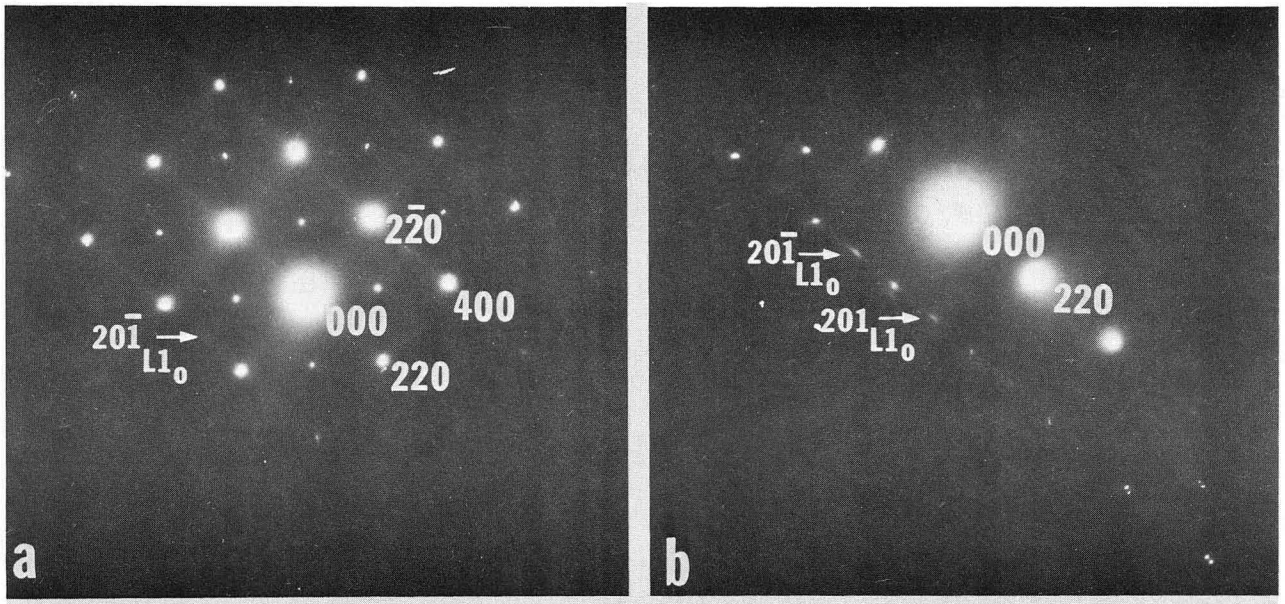

XBB 7211-5724

Fig. 2.

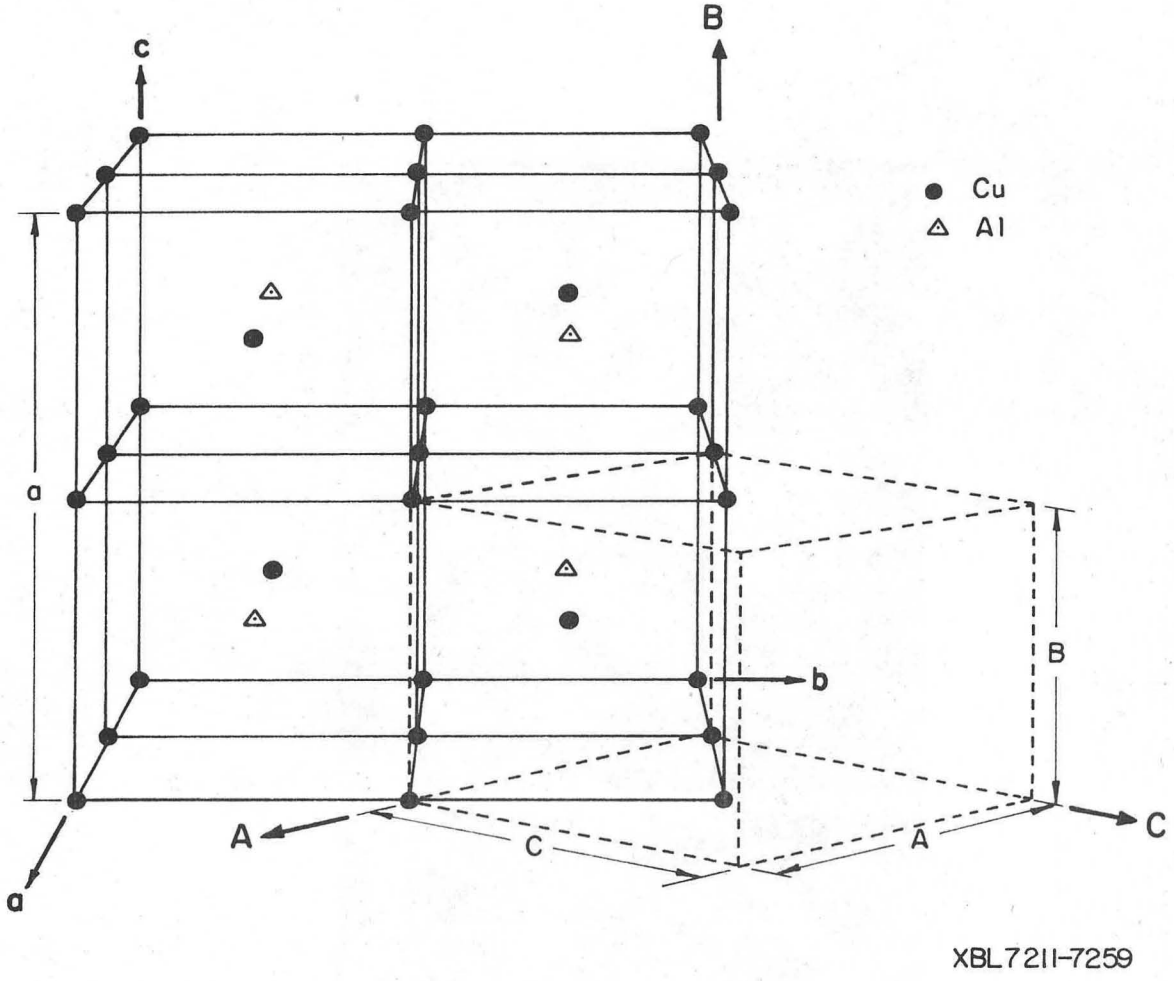

Fig. 3.

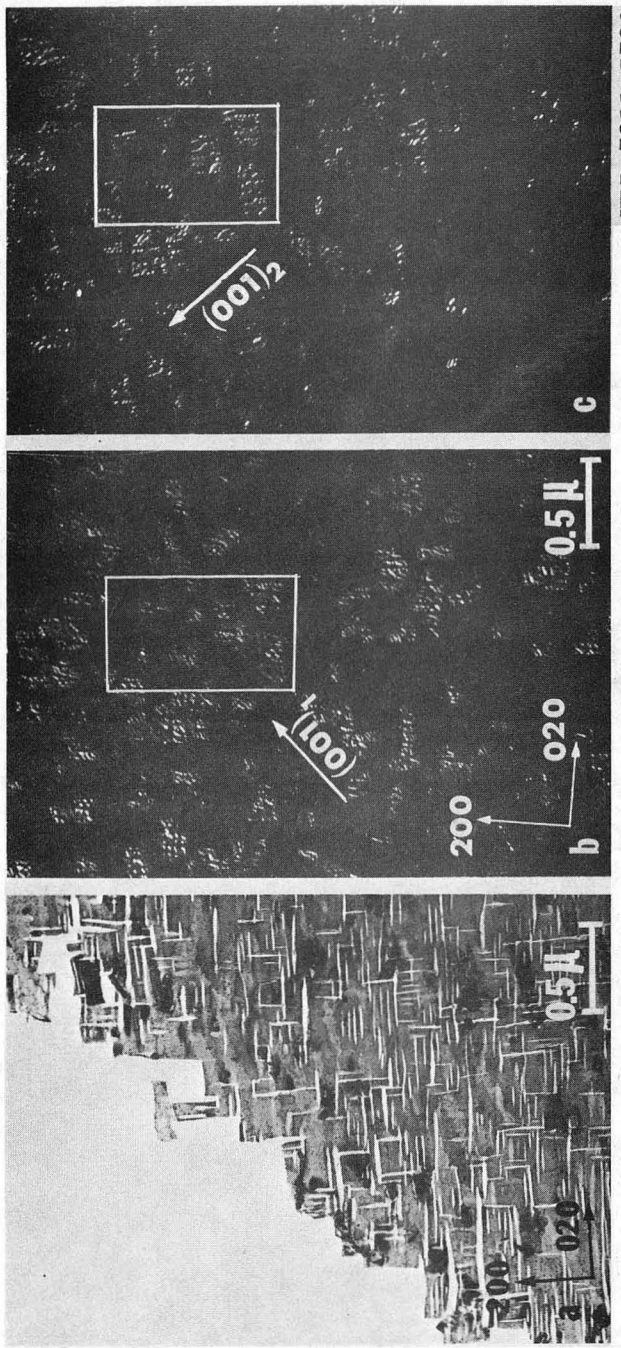

XBB 7211-5723

Fig. 4.

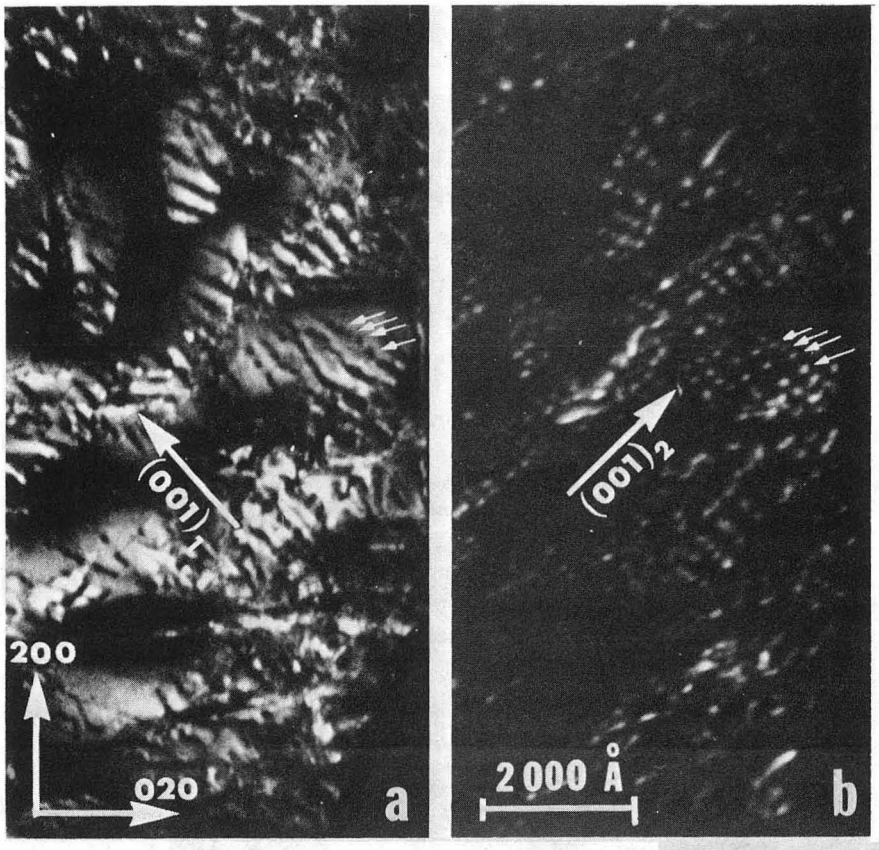

XBB 7211-5725

Fig. 5.

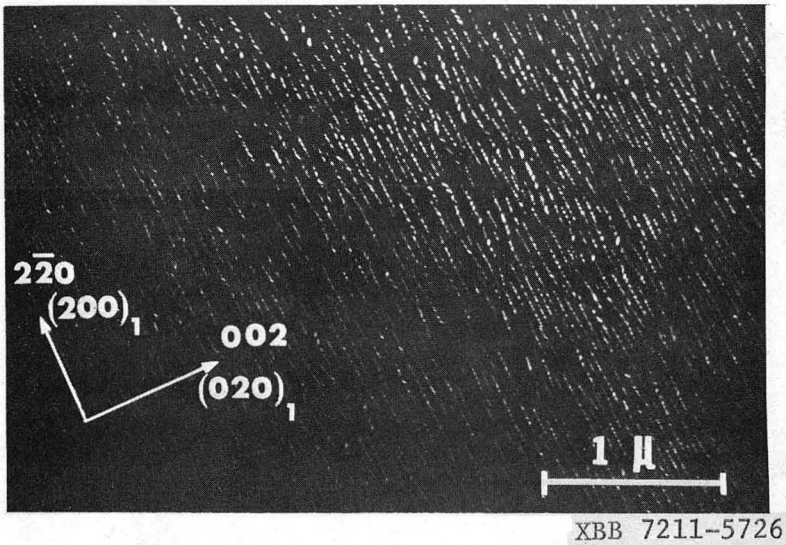

XBB 7211-5726

Fig. 6.

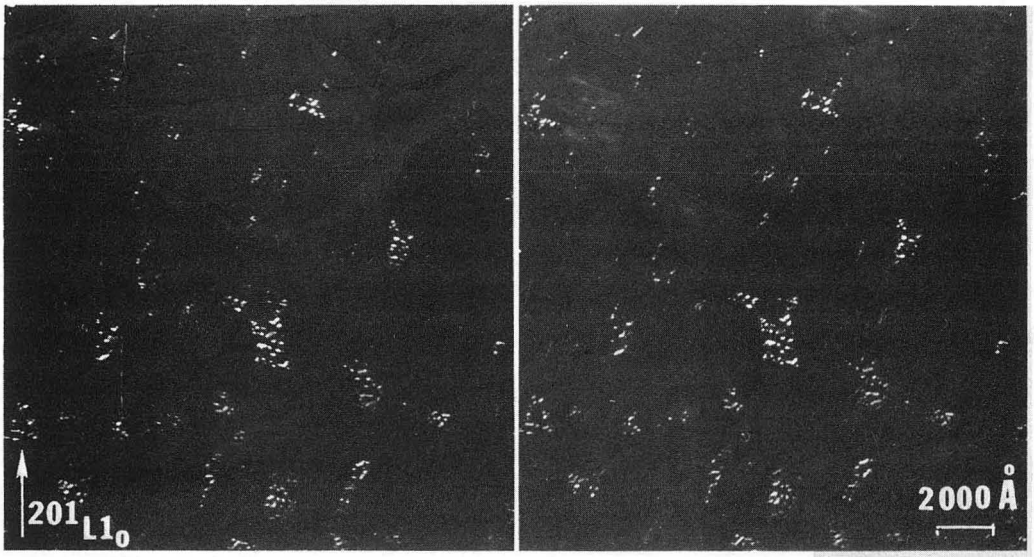

XBB 7211-5727

Fig. 7.

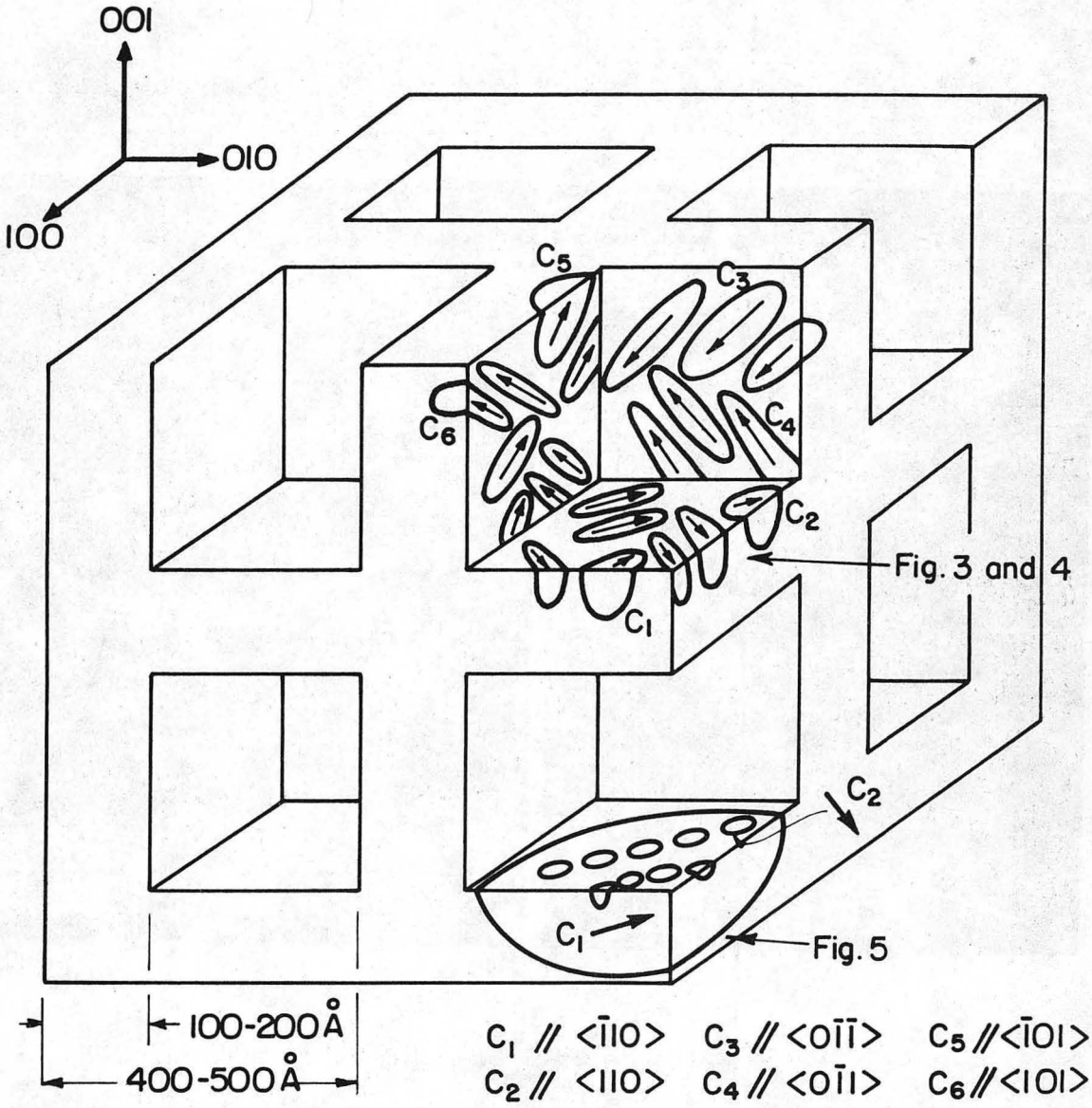
001
010
100
C5
C3
C6
C4
C2
Fig. 3 and 4
C1
C2
C1
Fig. 5
100-200 Å
400-500 Å
C1 // <1̄10> C3 // <01̄1̄> C5 // <1̄01>
C2 // <110> C4 // <01̄1> C6 // <101>
XBL7211-7264

Fig. 8.

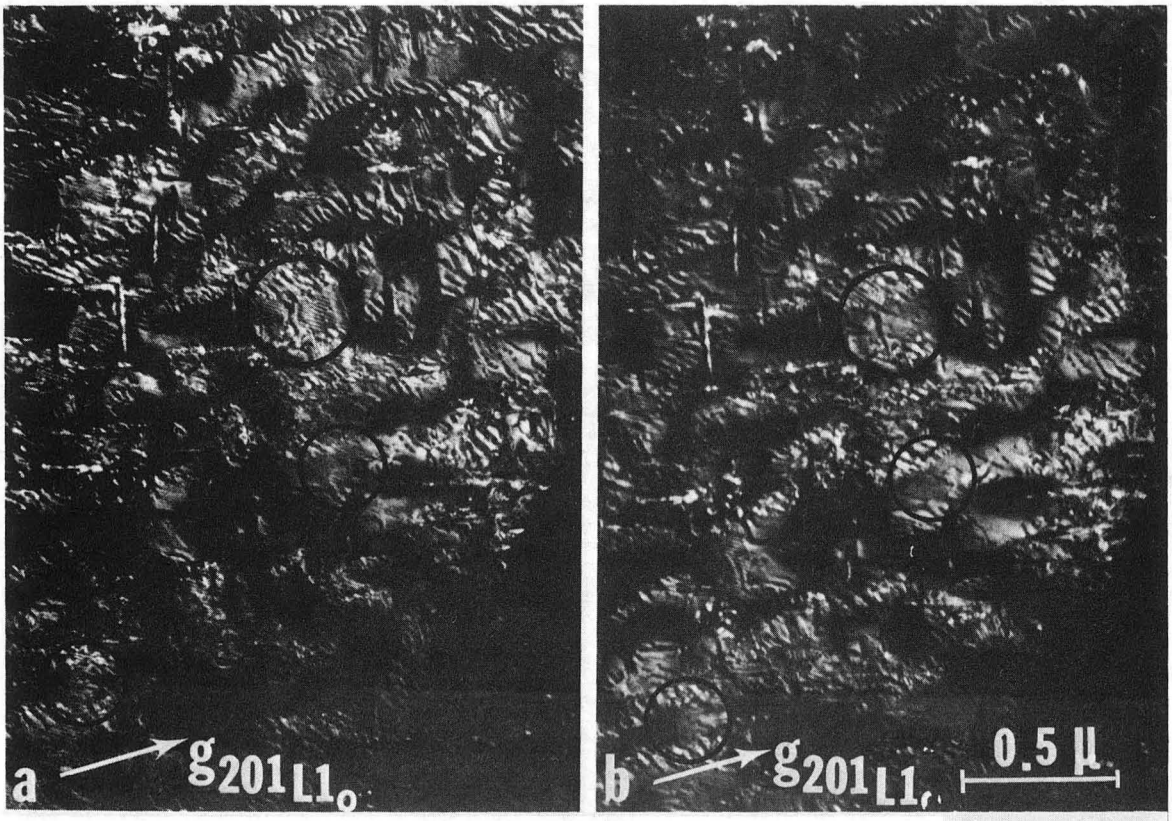

XBB 7211-5890

Fig. 9.

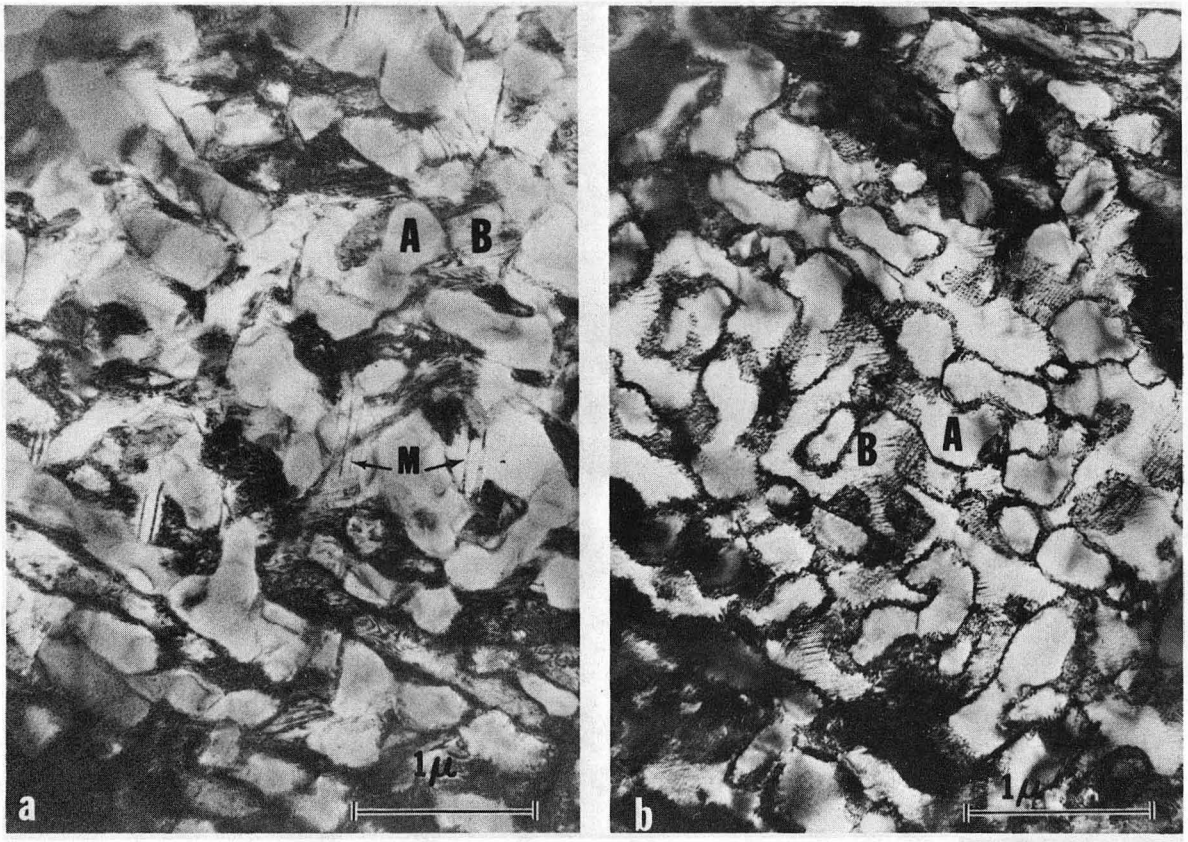

XBB 7211-5718

Fig. 10.

XBB 7211-5734

Fig. 11.

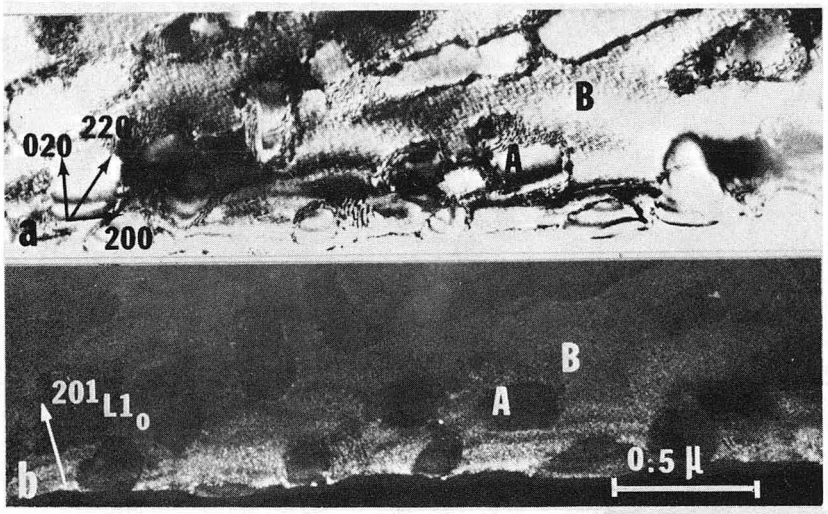

XBB 7211-5722

Fig. 12.

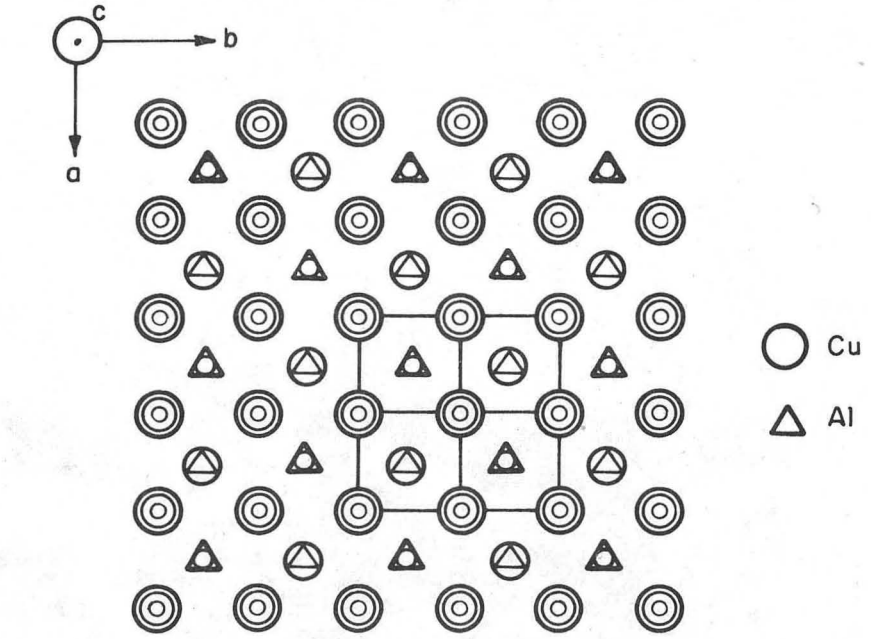

(a) DO_3 STRUCTURE

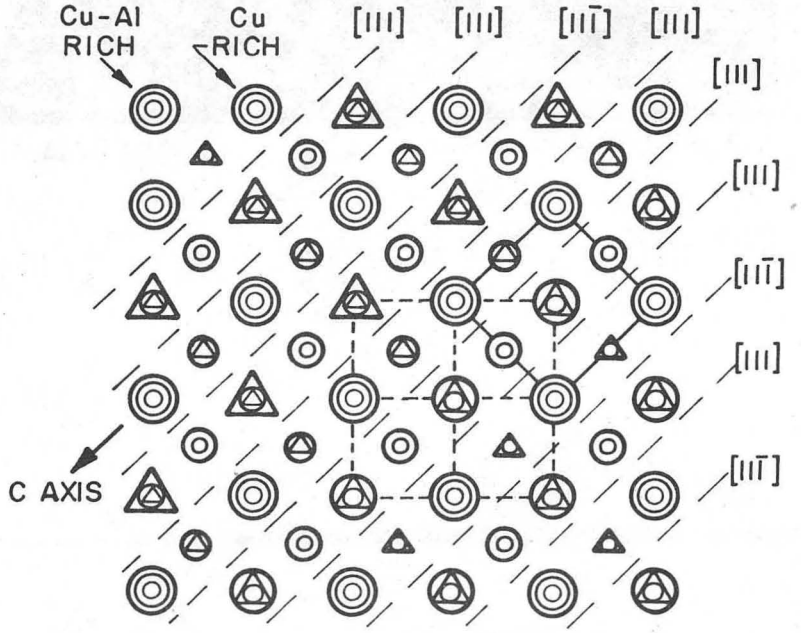

(b) LI_0 STRUCTURE

XBL7211-7265

Fig. 13.

TECHNICAL INFORMATION DIVISION
LAWRENCE BERKELEY LABORATORY
UNIVERSITY OF CALIFORNIA
BERKELEY, CALIFORNIA 94720